Journal of Power Sources 196 (2011) 8706–8709

Contents lists available at ScienceDirect

Journal of Power Sources

journal homepage: www.elsevier.com/locate/jpowsour

Short communication

Synthesis of plate-like $Li_3V_2(PO_4)_3$/C as a cathode material for Li-ion batteries

Y.Q. Qiao, X.L. Wang*, Y.J. Mai, J.Y. Xiang, D. Zhang, C.D. Gu, J.P. Tu*

State Key Laboratory of Silicon Materials and Department of Materials Science and Engineering, Zhejiang University, Hangzhou 310027, China

ARTICLE INFO

Article history:
Received 15 March 2011
Received in revised form 18 May 2011
Accepted 15 June 2011
Available online 22 June 2011

Keywords:
Lithium vanadium phosphate
Plate
Solution route
Lithium ion battery

ABSTRACT

Plate-like $Li_3V_2(PO_4)_3$/C composite is synthesized via a solution route followed by solid-state reaction. The $Li_3V_2(PO_4)_3$/C plates are 40–100 nm in thicknesses and 2–10 μm in lengths. TEM images show that a uniform carbon layer with a thickness of 5.3 nm presents on the surfaces of $Li_3V_2(PO_4)_3$ plates. The apparent Li-ion diffusion coefficient of the plate-like $Li_3V_2(PO_4)_3$/C is calculated to be 2.7×10^{-8} cm^2 s^{-1}. At a charge–discharge rate of 3 C, the plate-like $Li_3V_2(PO_4)_3$/C exhibits an initial discharge capacity of 125.2 and 133.1 mAh g^{-1} in the voltage ranges of 3.0–4.3 and 3.0–4.8 V, respectively. After 500 cycles, the electrodes still can deliver a discharge capacity of 111.8 and 97.8 mAh g^{-1} correspondingly, showing a good cycling stability.

1. Introduction

Monoclinic $Li_3V_2(PO_4)_3$ is considered to be one of the most promising cathode materials for lithium secondary batteries because of its advantages such as high operate voltage, high theoretical capacity (197 mAh g^{-1}) and good thermal stability [1,2]. Unfortunately, $Li_3V_2(PO_4)_3$ has an intrinsically low electronic conductivity (2.4×10^{-7} S cm^{-1}) as $LiFePO_4$ (10^{-10} to 10^{-9} S cm^{-1}) [3], which greatly limits its practical applications. Thereby, various methods have been used to solve this problem, including doping with foreign atoms [4–6], decreasing the particle size [2,7] and coating electronically conductive agents such as carbon [8–10] and Ag [11].

Numerous synthesis routes have been developed to prepare $Li_3V_2(PO_4)_3$, such as solid-state reaction [8–10,12], sol–gel method [2,13,14], rheological phase reaction [15], low temperature solid-state route [16], wet coordination method [17], microwave solid-state synthesis [18], hydrothermal synthesis [19], chemical reduction and lithiation method [20], and ultrasonic spray pyrolysis [21]. To date almost all the $Li_3V_2(PO_4)_3$ materials prepared by various methods are particulate composites, there are very few reports on $Li_3V_2(PO_4)_3$ with morphologies such as nanorods, nanobelts, nanoplates, and mesoporous structures. Recently, Liu et al. [22] synthesized $Li_3V_2(PO_4)_3$ nanorods with one-dimensional nanostructure by hydrothermal reaction, which showed good electrochemical performance due to the shorten distance of electron transport and ion diffusion in the nanorod radius. Moreover, nanostructured $Li_3V_2(PO_4)_3$/C with mesoporous carbon coating and the $Li_3V_2(PO_4)_3$/C thin film showed high reversible capacities, good capacity retention and high-rate capabilities [7,23]. More recently, Pan et al. [24] synthesized $Li_3V_2(PO_4)_3$ nanobelts by solid state reaction in a molten hydrocarbon, which showed good rate performance and excellent cycle stability. Electrode materials with plate-like characteristics could also exhibit excellent electrochemical performances [25–28]. Dokko et al. [28] synthesized $LiFePO_4$ with needle-like, plate-like and randomly shaped morphologies by changing the pH value using hydrothermal method, and they found that the plate-like crystals showed the highest electrochemical reactivity among the samples. Saravanan and co-workers [29–31] reported that the carbon-coated $LiFePO_4$ nanoplates exhibited impressive storage performance due to the nanoplate morphology favors short diffusion lengths for Li^+ ions along the *b*-axis. Choi et al. [32] and Wang et al. [33] demonstrated that nanoplate-like $LiMnPO_4$ could achieve a high specific capacity and excellent cycling ability. In this work, plate-like $Li_3V_2(PO_4)_3$/C is produced via a solution route followed by solid-state reaction. The electrochemical properties of the $Li_3V_2(PO_4)_3$/C composite are investigated, presenting a good electrochemical stability.

2. Experimental

The $Li_3V_2(PO_4)_3$/C composite was synthesized using a solution route followed by solid-state reaction. In a typical synthesis, 5.39 g of $LiOH{\cdot}H_2O$ and 4.00 g of glycine were dissolved in 30 mL of deionized water using two beakers under magnetic stirring, respectively. 10.00 g of NH_4VO_3 was added to another beaker with 50 mL of deionized water, then an appropriate quantity of H_3PO_4 (85%, solution) was added dropwise to the NH_4VO_3 turbid liquid under

* Corresponding authors. Tel.: +86 571 87952856; fax: +86 571 87952573.
E-mail addresses: wangxl@zju.edu.cn (X.L. Wang), tujp@zju.edu.cn (J.P. Tu).

0378-7753/$ – see front matter © 2011 Elsevier B.V. All rights reserved.
doi:10.1016/j.jpowsour.2011.06.056

magnetic stirring until a brownish-red solution was formed. Afterward, the resulting LiOH and glycine solution were added to the brownish-red solution gradually. And then, 0.80 g of carbon (Super P) was added to the mixed solution. After vigorous magnetic stirring at room temperature for 1 h, this mixed solution was dried in an oven at 70 °C to obtain the precursor. The precursor was then sintered at 700 °C for 10 h under Ar flow to get the $Li_3V_2(PO_4)_3$/C composite.

The morphology and microstructure of the as-synthesized powder were characterized using field emission scanning electron microscopy (FESEM, FEI SIRION), X-ray diffraction (XRD, Philips PC-APD with Cu Kα radiation) and high-resolution transmission electron microscopy (TEM, Tecnai G2 F30 S-Twin).

Electrochemical performances of the $Li_3V_2(PO_4)_3$/C composite were investigated using CR2025 coin-type cell. The cathode consisted of 85 wt.% active material, 10 wt.% carbon conductive agent (residual carbon and acetylene black) and 5 wt.% polyvinylidene fluoride on aluminum foil. A metallic lithium foil served as the anode. 1 M $LiPF_6$ in ethylene carbonate (EC)-dimethyl carbonate (DMC) (1:1 in volume) as the electrolyte, and a polypropylene micro-porous film (Cellgard 2300) as the separator. The cells were assembled in an argon-filled glove box. The charge–discharge tests were conducted on LAND battery program-control test system between 3.0 and 4.3 V, 3.0 and 4.8 V at rates of 0.1–3 C. Cyclic voltammetry (CV) were performed on CHI660 C electrochemical workstation in the potential ranges of 3.0–4.3 V and 3.0–4.8 V (vs. Li/Li^+) at scan rates from 0.05 to 0.25 mV s^{-1}, respectively.

3. Results and discussion

Fig. 1(a) and (b) depict the SEM images of the precursor and plate-like $Li_3V_2(PO_4)_3$/C, respectively. It is found that the precursor has plate-like morphology when glycine is used in solution synthesis (Fig. 1(a)). After sintering at 700 °C for 10 h, the particles still remain plate-like morphology (Fig. 1(b)). It is observed that the $Li_3V_2(PO_4)_3$/C plates have 40–150 nm in thicknesses. The lengths of the plates are not uniform and they are in the range of 2–10 μm. It is known that $Li_3V_2(PO_4)_3$ is an insulator for both of lithium ions and electrons, thus it is worth of establishing a uniform carbon layer on $Li_3V_2(PO_4)_3$ particle in order to improve its electrochemical performance. From XRD analysis, all the diffraction peaks of the as-synthesized powder can be indexed as monoclinic $Li_3V_2(PO_4)_3$ phase (space group $P2_1/n(14)$, ICSD #96962), as shown in Fig. 1(c). There is no evidence in the XRD pattern for the presence of carbon due to its low content or amorphous state in the composite. The carbon content in the plate-like $Li_3V_2(PO_4)_3$/C is 3.22 wt.% according to the elemental analysis. It is also noticed that the peak intensity ratios of $I_{(020)}/I_{(220)}$ and $I_{(020)}/I_{(\bar{3}11)}$ are 1.87 and 3.86, respectively, while the granular $Li_3V_2(PO_4)_3$ are in the ranges of 1.23–1.38 and 1.97–2.81 [1,7,22], respectively. This also suggests that the particles have some preferred crystal orientation such as plate-like morphology. From the TEM images of the plate-like $Li_3V_2(PO_4)_3$/C, as shown in Fig. 1(d)–(f), a uniform carbon layer presents on the surfaces of $Li_3V_2(PO_4)_3$ plates, similar to the carbon-coated $LiFePO_4$ nanoplates [29]. It can be found that the thickness of the carbon layer is about 5.3 nm (Fig. 1(f)). In the body part of the particle, the lattice fringes are clearly visible, indicating single crystallinity of the plate. The 6.94 Å spacing corresponds to the (1 1 0) plane of monoclinic $Li_3V_2(PO_4)_3$.

Fig. 2(a) and (b) show the initial charge–discharge profiles of plate-like $Li_3V_2(PO_4)_3$/C at 0.1 C and the corresponding differential capacity plots. The differential capacity plots derived by the data of charge–discharge at 0.1 C, and the characteristics of the plots are indicative of the complex insertion-extraction reactions of the Li ions for the electrode [1–3]. The plate-like $Li_3V_2(PO_4)_3$/C demonstrates a specific capacity of 131.6 mAh g^{-1} between 3.0 and 4.3 V at 0.1 C (99% of the theoretical capacity), while in the potential range of 3.0–4.8 V, the electrode displays a high discharge capacity

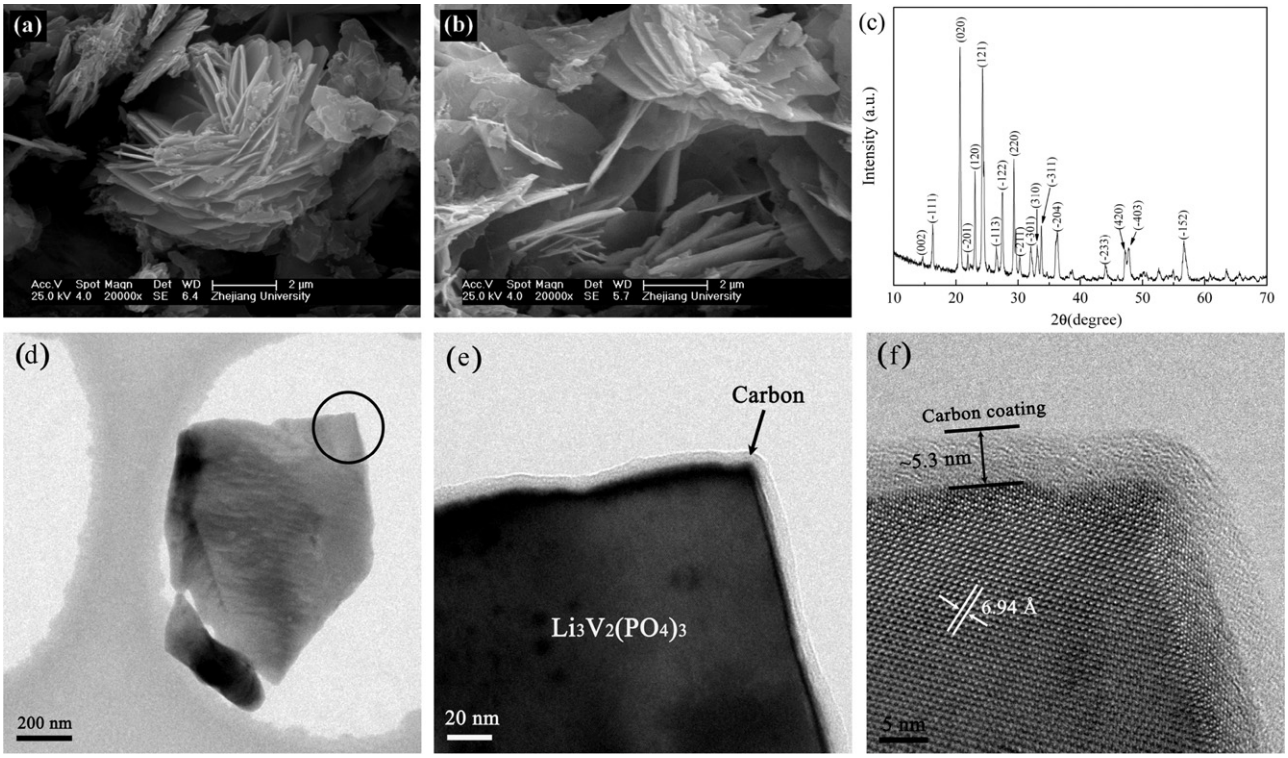

Fig. 1. SEM images of (a) precursor and (b) plate-like $Li_3V_2(PO_4)_3$/C; (c) XRD pattern of $Li_3V_2(PO_4)_3$/C. (d) TEM image of plate-like $Li_3V_2(PO_4)_3$/C. (e) An enlarged TEM image showing a uniform coverage of amorphous carbon layer on the surface of $Li_3V_2(PO_4)_3$ (indicated by a circle in panel d), and (f) A HRTEM image showing nearly 5.3-nm thick amorphous carbon layer on the surface of $Li_3V_2(PO_4)_3$ particle and lattice fringes of monoclinic $Li_3V_2(PO_4)_3$.

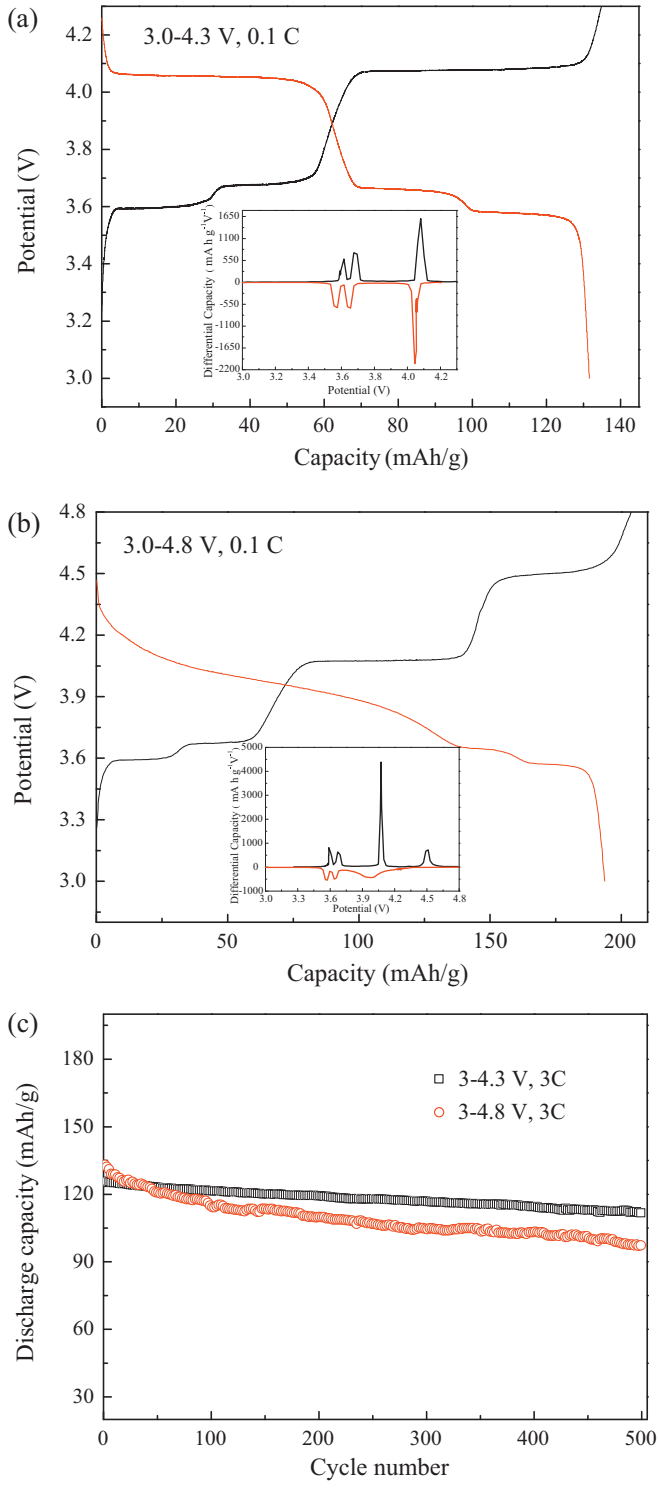

Fig. 2. The initial charge–discharge profiles of plate-like $Li_3V_2(PO_4)_3$/C in the voltage ranges of (a) 3.0–4.3 V and (b) 3.0–4.8 V at 0.1 C, and the corresponding differential capacity plots. (c) Cycling performance at 3 C.

of 193.7 mAh g^{-1} (98% of the theoretical capacity). Fig. 2(c) shows the cycling performance of the plate-like $Li_3V_2(PO_4)_3$/C at 3 C. It can be found that the plate-like $Li_3V_2(PO_4)_3$/C has an initial discharge capacity of 125.2 and 133.1 mAh g^{-1} at 3 C in the voltage ranges of 3.0–4.3 and 3.0–4.8 V, respectively. Even after 500 cycles, discharge capacities of 111.8 and 97.8 mAh g^{-1} can still be sustained at 3 C between 3.0 and 4.3 V, and 3.0–4.8 V, respectively. The cell retains

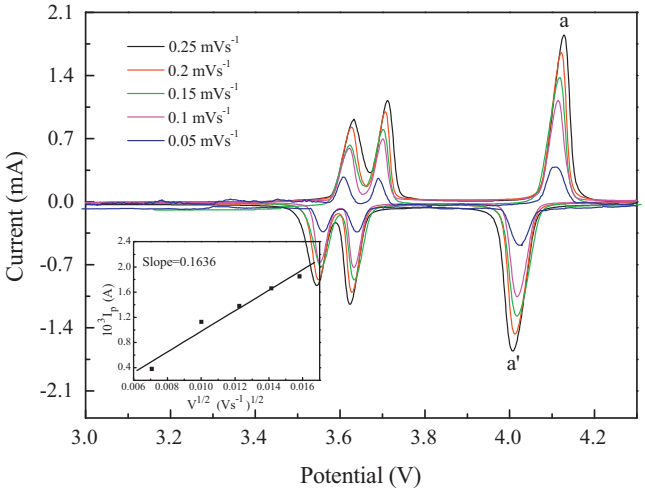

Fig. 3. CV curves for plate-like $Li_3V_2(PO_4)_3$/C at scan rates from 0.05 to 0.25 mV s^{-1}.

89.3% and 66.0% of its initial discharge capacity correspondingly, showing a good cycling performance.

Fig. 3 shows CV curves of the plate-like $Li_3V_2(PO_4)_3$/C at different scan rates. The symmetrical and well-defined oxidation and reduction peaks in the CV plots indicate the good reversibility of lithium extraction/insertion reactions in the material. For the semi-infinite and finite diffusion, the relationship between the peak current and the square root of scan rate are used to extract the Li-ion diffusion coefficient, applying the Randles Sevcik equation [8,10]:

$$I_p = 2.69 \times 10^5 n^{3/2} A D^{1/2} C v^{1/2}$$

where I_p is the peak current (A), n is the number of electrons per species reaction, A is the contact area between $Li_3V_2(PO_4)_3$/C and electrolyte (here the geometric area of electrode, 1.0 cm^2, is used for simplicity), D is the diffusion coefficient of Li^+ in the solid state (cm^2 s^{-1}), C is the shuttle concentration (3.7×10^{-3} mol cm^{-3} [10]), and v is the potential scan rate (V s^{-1}). From the slope of the linear fit (insert graph in the bottom left corner in the panel), the apparent Li-ion diffusion coefficient of the plate-like $Li_3V_2(PO_4)_3$/C is calculated to be 2.7×10^{-8} cm^2 s^{-1}. It is found that the value of D_{Li+} is very close to the value (the order of 10^{-9} cm s^{-1}) reported by Huang et al. [34], and are higher than the ones obtained by other research groups [8,17]. This fast ionic conductivity character favors fast rate and power applications.

4. Conclusions

Plate-like $Li_3V_2(PO_4)_3$/C composite was successfully synthesized via a solution route followed by solid-state reaction. The $Li_3V_2(PO_4)_3$ plates were coated by a uniform carbon layer with a thickness of 5.3 nm. The plate-like $Li_3V_2(PO_4)_3$/C exhibited an initial discharge capacity of 125.2 and 133.1 mAh g^{-1} at 3 C in the voltage ranges of 3.0–4.3 and 3.0–4.8 V, respectively. After 500 cycles, 89.3% and 66.0% of its initial discharge capacity could be maintained correspondingly, showing a good cycling performance.

References

[1] S.-C. Yin, H. Grondey, P. Strobel, M. Anne, L.F. Nazar, J. Am. Chem. Soc. 125 (2003) 10402.
[2] H. Huang, S.-C. Yin, T. Kerr, N. Taylor, L.F. Nazar, Adv. Mater. 14 (2002) 1525.
[3] S.-C. Yin, P.S. Strobel, H. Grondey, L.F. Nazar, Chem. Mater. 16 (2004) 1456.
[4] C.S. Dai, Z.Y. Chen, H.Z. Jin, X.G. Hu, J. Power Sources 195 (2010) 5775.
[5] Y.H. Chen, Y.M. Zhao, X.N. An, J.M. Liu, Y.Z. Dong, L. Chen, Electrochim. Acta 54 (2009) 5844.
[6] J.S. Huang, L. Yang, K.Y. Liu, Y.F. Tang, J. Power Sources 195 (2010) 5013.

[7] A.Q. Pan, J. Liu, J.-G. Zhang, W. Xu, G.Z. Cao, Z.M. Nie, B.W. Arey, S.Q. Liang, Electrochem. Commun. 12 (2010) 1674.
[8] X.H. Rui, N. Ding, J. Liu, C. Li, C.H. Chen, Electrochim. Acta 55 (2010) 2384.
[9] Y.Q. Qiao, X.L. Wang, Y. Zhou, J.Y. Xiang, D. Zhang, S.J. Shi, J.P. Tu, Electrochim. Acta 56 (2010) 510.
[10] T. Jiang, W.C. Pan, J. Wang, X.F. Bie, F. Du, Y.J. Wei, C.Z. Wang, G. Chen, Electrochim. Acta 55 (2010) 3864.
[11] L. Zhang, X.L. Wang, J.Y. Xiang, Y. Zhou, S.J. Shi, J.P. Tu, J. Power Sources 195 (2010) 5057.
[12] Y.Q. Qiao, X.L. Wang, J.Y. Xiang, D. Zhang, W.L. Liu, J.P. Tu, Electrochim. Acta 56 (2011) 2269.
[13] X.J. Zhu, Y.X. Liu, L.M. Geng, L.B. Chen, J. Power Sources 184 (2008) 578.
[14] Y.Z. Li, X. Liu, J. Yan, Electrochim. Acta 53 (2007) 474.
[15] C.X. Chang, J.F. Xiang, X.X. Shi, X.Y. Han, L.J. Yuan, J.T. Sun, Electrochim. Acta 53 (2008) 2232.
[16] L.J. Wang, X.C. Zhou, Y.L. Guo, J. Power Sources 195 (2010) 2844.
[17] L. Wang, X.Q. Jiang, X. Li, X.Q. Pi, Y. Ren, F. Wu, Electrochim. Acta 55 (2010) 5057.
[18] G. Yang, H.M. Ji, H.D. Liu, B. Qian, X.F. Jiang, Electrochim. Acta 55 (2010) 3669.
[19] C.X. Chang, J.F. Xiang, X.X. Shi, X.Y. Han, L.J. Yuan, J.T. Sun, Electrochim. Acta 54 (2008) 623.
[20] J.C. Zheng, X.H. Li, Z.X. Wang, H.J. Guo, Q.Y. Hu, W.J. Peng, J. Power Sources 189 (2009) 476.
[21] Y.Na. Ko, H.Y. Koo, J.H. Kim, J.H. Yi, Y.C. Kang, J.-H. Lee, J. Power Sources 196 (2011) 6682.
[22] H.W. Liu, C.X. Cheng, X.T. Huang, J.L. Li, Electrochim. Acta 55 (2010) 8461.
[23] L. Wang, L.C. Zhang, I. Lieberwirth, H.W. Xuand, C.H. Chen, Electrochem. Commun. 12 (2010) 52.
[24] A.Q. Pan, D. Choi, J.-G. Zhang, S.Q. Liang, G.Z. Cao, Z.M. Nie, B.W. Arey, J. Liu, J. Power Sources 196 (2011) 3646.
[25] G. Chen, X. Song, T.J. Richardson, Electrochem, Solid State Lett. 9 (2006) A295.
[26] S. Ferrari, R.L. Lavall, D. Capsoni, E. Quartarone, A. Magistris, P. Mustarelli, P. Canton, J. Phys. Chem. C 114 (2010) 12598.
[27] X. Qin, X.H. Wang, H.M. Xiang, J. Xie, J.J. Li, Y.C. Zhou, J. Phys. Chem. C 114 (2010) 16806.
[28] K. Dokko, S. Koizumi, H. Nakano, K. Kanamura, J. Mater. Chem. 17 (2007) 4803.
[29] K. Saravanan, M.V. Reddy, P. Balaya, H. Gong, B.V.R. Chowdari, J.J. Vittal, J. Mater. Chem. 19 (2009) 605.
[30] K. Saravanan, P. Balaya, M.V. Reddy, B.V.R. Chowdaric, J.J. Vittal, Energy Environ. Sci. 3 (2010) 457.
[31] K. Saravanan, J.J. Vittal, M.V. Reddy, B.V.R. Chowdari, P. Balaya, J. Solid State Electrochem. 14 (2010) 1755.
[32] D. Choi, D. Wang, I.T. Bae, J. Xiao, Z. Nie, W. Wang, V.V. Viswanathan, Y.J. Lee, J.-G. Zhang, G.L. Graff, Z. Yang, J. Liu, Nano Lett. 10 (2010) 2799.
[33] D. Wang, H. Buqa, Mi. Crouzet, G. Deghenghi, T. Drezen, I. Exnar, N.-H. Kwon, J.H. Miners, L. Poletto, M. Grätzel, J. Power Sources 189 (2009) 624.
[34] H. Huang, T. Faulkner, J. Barker, M.Y. Saidi, J. Power Sources 189 (2009) 748.